Monte Carlo simulation of diffusion controlled colloid growth rates in two and three dimensions

Paul Meakin
Central Research and Development Department,[a]
Experimental Station, E. I. du Pont de Nemours and Company, Wilmington, Delaware 19898

J. M. Deutch[b]
Department of Chemistry, Massachusetts Institute of Technology, Cambridge, Massachusetts 02139

(Received 13 September 1983; accepted 23 November 1983)

The kinetics of diffusion limited aggregation have been explored in two and three dimensions using Monte Carlo simulations. If the initial particle concentration is very low, our model is equivalent to the Witten–Sander model of diffusion limited aggregation, and the resulting cluster has a Hausdorff dimensionality (D) substantially lower than the ordinary Euclidean dimensionality (d) ($D \simeq 5d/6$). Under these conditions, the radius of gyration (R_g) of the clusters grows according to the rate law $R_g(t) \sim t^{[1/(2+D-d)]}$ obtained previously. If the initial particle concentration is large, the radius of gyration increases linearly with time, and the clusters are uniform ($D = d$) on all but very short length scales. In general, the clusters grow like Witten–Sander clusters during the early stages of growth. As the clusters grow larger and larger, they become less and less dense until their density approaches that of the surrounding medium. At this stage of growth, there is a crossover from a growth exponent of $1/(2+D-d)$ for R_g to linear growth, and the dependence of the radius of gyration on cluster size crosses over from $R_g \sim N^{\beta}$ ($\beta \simeq 6/5d$) to $R_g \sim N^{\beta'}$ ($\beta' = 1/d$). The structure of the cluster is Witten–Sander-like on short length scales but uniform on long length scales. At no stage does the cluster growth follow the classical $t^{1/2}$ behavior. In two dimensional space, the rate of increase of *mass* is given by $N(t) \sim t$ for diffusion limited aggregation in the early stages of growth.

I. INTRODUCTION

Witten and Sander[1] have recently developed a model for diffusion limited aggregation which leads to complex random dendritic structures. Numerical simulations using the Witten–Sander (WS) model indicate that these structures possess interesting scaling and universality properties.[1,2] These results and recent work on other models[3–5] have stimulated considerable theoretical[6–11] and experimental interest[12] in the relationship(s) between growth mechanisms and morphology particularly in those cases where the resulting structures have a fractal[13] geometry.

It has recently been shown that WS clusters develop in time according to the growth law

$$R(t) \sim t^{[1/(2+D-d)]}, \tag{1}$$

where $R(t)$ is the mean radius of the cluster at time t, d is the (ordinary) Euclidean dimensionality of the cluster, and D is the Hausdorff[14] (fractal[13]) dimensionality of the cluster. We[15] have derived Eq. (1) subject to the conditions $d > 3$ and $(d - D) < 2$. Similar results have been obtained by Witten for $d = 3$.[16] The easiest way[15] to derive Eq. (1) is to determine the flux of material entering the cluster from the steady state concentration profile using the diffusion equation

$$D \frac{1}{r^{d-1}} \frac{d}{dr} r^{d-1} \frac{dC(r,t)}{dr} = \frac{dC(r,t)}{dt} = 0 \quad \text{(at steady state)}, \tag{2}$$

where $C(r,t)$ is the concentration profile at time t. For $d \leqslant 2$, the concentration profile does not reach a steady state, and this approach cannot be used.

For the case of three dimensional clusters, we have found from numerical simulations[2] that the Hausdorff dimensionality (D) has a value of ~ 2.5. For an aggregate with a Hausdorff dimensionality of 2.5 growing under diffusion limited conditions, Eq. (1) gives

$$R_g(t) \sim t^{(2/3)}, \tag{3}$$

where R_g is the radius of gyration at time t. Since $N \sim R_g^D$, we also expect that

$$N(t) \sim t^{(5/3)}. \tag{4}$$

Similarly, for diffusion limited aggregation in two dimensions[1,2] $D \simeq 5/3$. If D is exactly 5/3 and if Eq. (1) is applied in $d = 2$, we expect that

$$R_g(t) \sim t^{(3/5)} \tag{5}$$

and

$$N(t) \sim t^{1.0}. \tag{6}$$

The main objective of this paper is to test Eqs. (3)–(6).

The simulations (described below) were carried out for finite systems with a nonzero (small in most cases) concentration of particles. After an initial transient, we expect the clusters to grow according to Eqs. (3) and (4) for $d = 3$ or Eqs. (5) and (6) for $d = 2$. As the clusters grow larger and larger, their density becomes smaller and smaller until the density of the cluster approaches the average density of the particles in the medium. During the early stages of growth, the clusters should be very similar to those grown according to the WS method.[1] Consequently, we expect that $R_g \sim N^{1/D}$ and $C(r) \sim r^{D-d}$ where $C(r)$ is the density–density correla-

[a] Contribution No. 3305.
[b] Supported in part by the National Science Foundation.

 0021-9606/84/052115-08$02.10

tion function. Density–density correlation functions obtained from the model used in this paper (for $d = 2$) have been described previously.[17]

As the density of the clusters approaches the density of the particle bath, both the rate of growth of the radius of gyration and the morphology of the clusters will change. After passing through a "crossover" region, we expect to find that

$$R_g(t) \sim t \quad \text{(for all } d\text{)} \tag{7}$$

and

$$N(t) \sim t^d \quad \text{(for all } d\text{)}. \tag{8}$$

In the final stage, the cluster growth will deplete the particles and growth will slow down rapidly.

II. SIMULATION METHODS

The simulations used in connection with the work described in this paper were carried out using two dimensional or three dimensional lattice models. The simulation starts with a single stationary occupied site or "seed" at the center of a square or simple cubic lattice. A large number of mobile sites or "particles" are then added at random to unoccupied sites of the lattice. Diffusion of the particles is represented by a series of jumps to nearest neighbor sites. One of the particles is selected at random and an attempt is made to move it to one of its nearest neighbor sites (also selected at random). If the particle moves to a site which is adjacent to the seed or adjacent to a particle which is attached to the seed by a series of occupied lattice sites (i.e., a particle which is part of a growing cluster), it remains stationary and becomes part of the cluster. If the attempted move would transfer the particle to a site already occupied by a particle, the move is not made and another particle is selected (we do not allow more than one particle to occupy a single lattice site). Once a particle has been incorporated into the cluster, all other particles which are in its nearest neighbor sites and all other particles which are connected to it via a series of nearest neighbor sites also become part of the cluster. Periodic boundary conditions are used in these simulations.

A running sum of successful and unsuccessful moves per particle is kept as a measure of "time" in these simulations. Most of our calculations have been carried out with a single seed particle, but some results were also obtained with either an ordered or random array of multiple growth sites.

III. RESULTS

A. Two dimensional simulations

Figure 1 shows some of the results of a simulation which was started with a single stationary seed particle and 20 000 mobile particles on a 400×400 lattice [i.e., initial particle concentration (ρ) of 0.125 particles per lattice site]. During the initial stages of growth, the cluster closely resembles clusters obtained using the WS model. For example, Figs. 1(a) and 1(b) show the cluster after 1000 and 5000 particles have been added. Even after 10 000 particles have been added [Figure 1(c)], the cluster still resembles a Witten–Sander cluster. However, at this stage the cluster is significantly denser than a WS cluster of the same size. In most of the simulations we have carried out using the WS model, the cluster has approached very close to the edges of a 400×400 lattice or reached beyond the edges after 10 000 particles have been added. After 20 000 particles have been added [Figure 1(d)], the cluster has grown beyond the edges of the 400×400 lattice. Figure 2 shows the results of a similar simulation in which 40 000 mobile particles were added to a single seed on a 400×400 lattice ($\rho = 0.25$). Figure 2(a) shows the cluster after 1000 particles have been added. It is quite similar to that shown in Fig. 1(a) and also similar to a WS cluster of 1000 particles. In Figure 2(b), 5000 of the 40 000 particles have been added to the cluster. At this stage, the cluster is noticeably more compact than the cluster shown in Fig. 1(b) and also more compact than a WS cluster of 5000 particles. By the time cluster has grown to a size of 10 000 particles [Figure 2(c)], it has become apparent that the structure is quite uniform on all but small length scales. Figure 2(d) shows the cluster after 20 000 (50%) of the mobile particles have been added to the cluster.

Figure 3 shows the dependence of $\ln(R_g)$ on $\ln(N)$ during simulations in which 10 000 (curve A, 20 000 (B), 40 000 (C), and 50 000 (D) particles were added to a single growth site on a 400×400 square lattice. The corresponding initial concentrations ρ are 0.0625, 0.125, 0.25, and 0.3125 particles per lattice site. At an initial concentration of 0.0625, the cluster resembles a WS cluster throughout its entire growth, and we find that $R_g \sim N^{\beta}$ ($\beta \approx 0.6$). For the simulation starting at a concentration of 0.125 (B), the initial growth is very much like that of a WS cluster, but there are noticeable deviations towards the later stages. The dependence of $\ln(R_g)$ on $\ln(N)$ is not completely linear. Part of the nonlinearity may be because of the folding about the edges of the lattice to represent the growth into adjacent lattice images which is not taken into account in calculating R_g. At larger concentrations (curves C and D), the transition from WS growth to a more uniform growth process occurs at much earlier stages, and we find that $R_g \sim N^{1/2}$ for large clusters. The curves C and D clearly exhibit crossover behavior from the nonclassical WS growth to classical growth of a compact structure as the concentration difference between the cluster and the medium decreases. In our opinion, there as yet is not an adequate theoretical explanation for this crossover behavior.

The main objective of our simulations was to explore growth rates in diffusion limited aggregation. Figure 4 shows the dependence of R_g on "time" (number of Monte Carlo steps per particle) for simulations carried out under the same conditions which were used to obtain the results shown in Fig. 3. To facilitate comparison with Eqs. (5) and (7), dashed lines with slopes of 3/5 and 1.0 have been drawn in Fig. 4. For curve A ($\rho = 0.0625$), the growth of the radius of gyration is described quite well by Eq. (5) throughout most of the simulation (i.e., $R_g \sim t^{3/5}$). For curve B ($\rho = 0.125$), the growth of the radius of gyration also has an exponent of about 5/3 throughout most of the simulation. However, in this case the slope increases as the cluster density approaches the density of the growth medium and decreases quite sharply as the particles are depleted. For the simulation carried out at an initial density of $\rho = 0.25$ (curve C), there is a clear

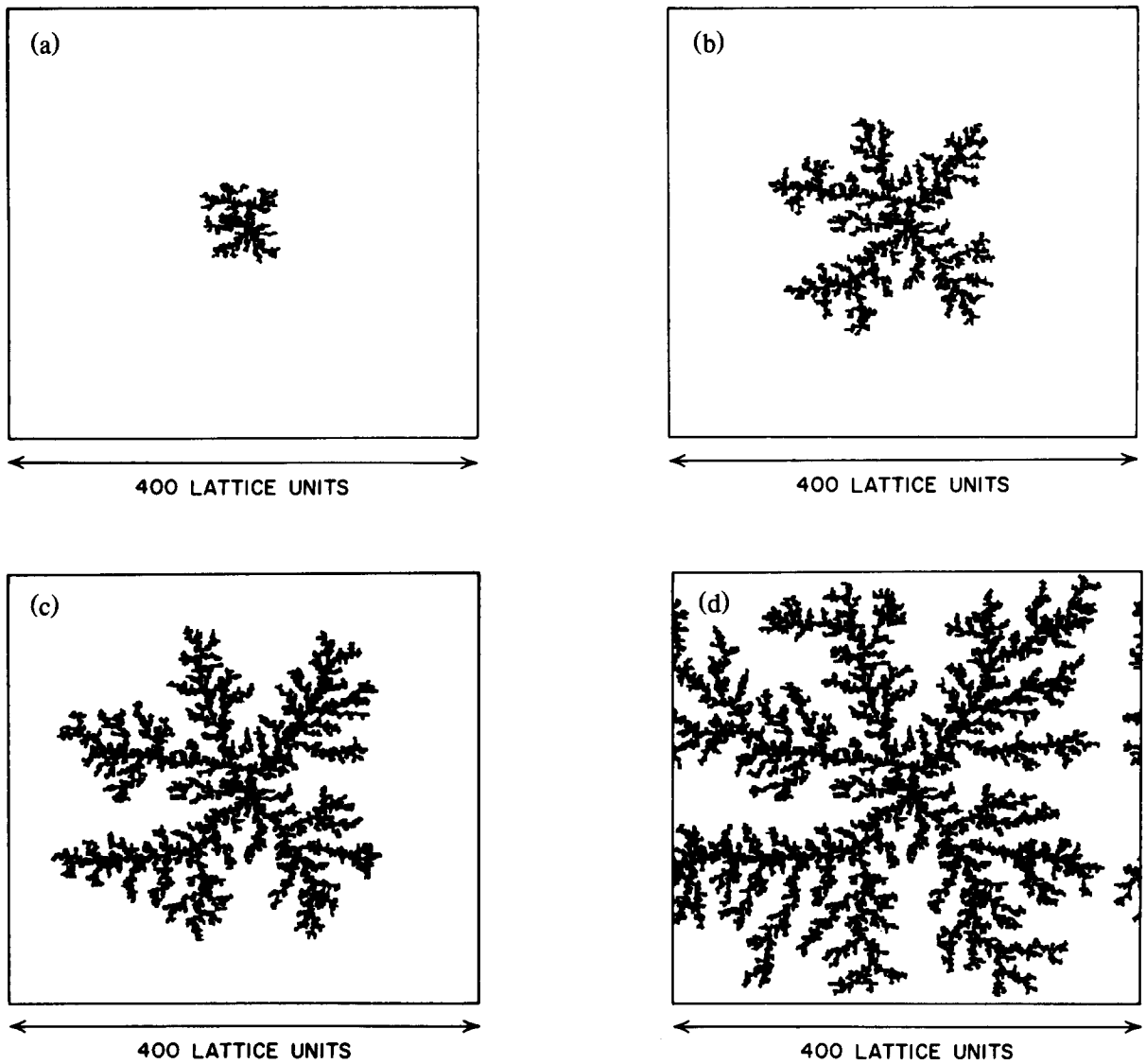

FIG. 1. Growth of a two-dimensional cluster from an initial state containing one seed or growth site and 20 000 mobile sites or particles on a 400×400 lattice. (a) At this stage in the simulation 1000 particles have been added to the original seed. This cluster closely resembles a typical cluster of 1000 particles grown using the WS model for diffusion limited aggregation. (b) Five thousand particles have now been added to the cluster which still closely resembles a WS cluster of the same size (number of particles). (c) This figure shows a cluster of 10 000 particles. The cluster still resembles a Witten–Sander cluster but is substantially denser. (d) All 20 000 mobile particles have now been added. The cluster has grown into the periodic lattice images and growth from adjacent lattice images can be seen in this figure.

crossover from $t^{3/5}$ to t^{1} behavior. Curve D is the average of the results of six simulations. The density is quite high ($\rho = 0.3125$). Consequently, some quite large "temporary" clusters exist during the simulation and statistical fluctuations become much larger than in simulations carried out at lower densities. However, curves C and D together provide quite strong support for t^{1} growth of the radius of gyration at large cluster sizes.

Figure 5 shows the growth of the mass (number of particles) obtained from the simulations which were used to produce Fig. 4. Curves A and B, obtained at relatively low concentrations, agree with the t^{1} growth predicted by Eq. (6). Similarly, curves C and D show a crossover to t^{2} behavior for higher concentrations and/or large cluster sizes. Again, the crossover is seen most clearly in curve C (40 000 particles, $\rho = 0.25$).

Simulations have also been carried out using more than one seed or growth site. Figure 6 shows the dependence of N (the number of particles added to any of the seeds) as a function of time during four simulations at four different concentrations with 50 seeds on a 400×400 lattice. Curves A and B correspond to relatively low concentrations ($\rho = 0.062$ and 0.125 particles per lattice site, respectively). The dependence of N and t can be described approximately by a power law with an exponent slightly larger than the theoretical value of 1.0 at intermediate times. At larger concentrations ($\rho = 0.25$ for curve C and 0.3125 for curve D), the slope in the plots of $\ln(N)$ vs $\ln(t)$ is larger but does not approach the theoretical value of 2.0. One reason for this is that the clusters are relatively small and "interfere" with each other's growth.[17] As clusters approach each other, the effective concentration at the cluster/medium interface is reduced below that which would be found if the clusters were very far from each other. A similar competitive phenomenon occurs in classical diffu-

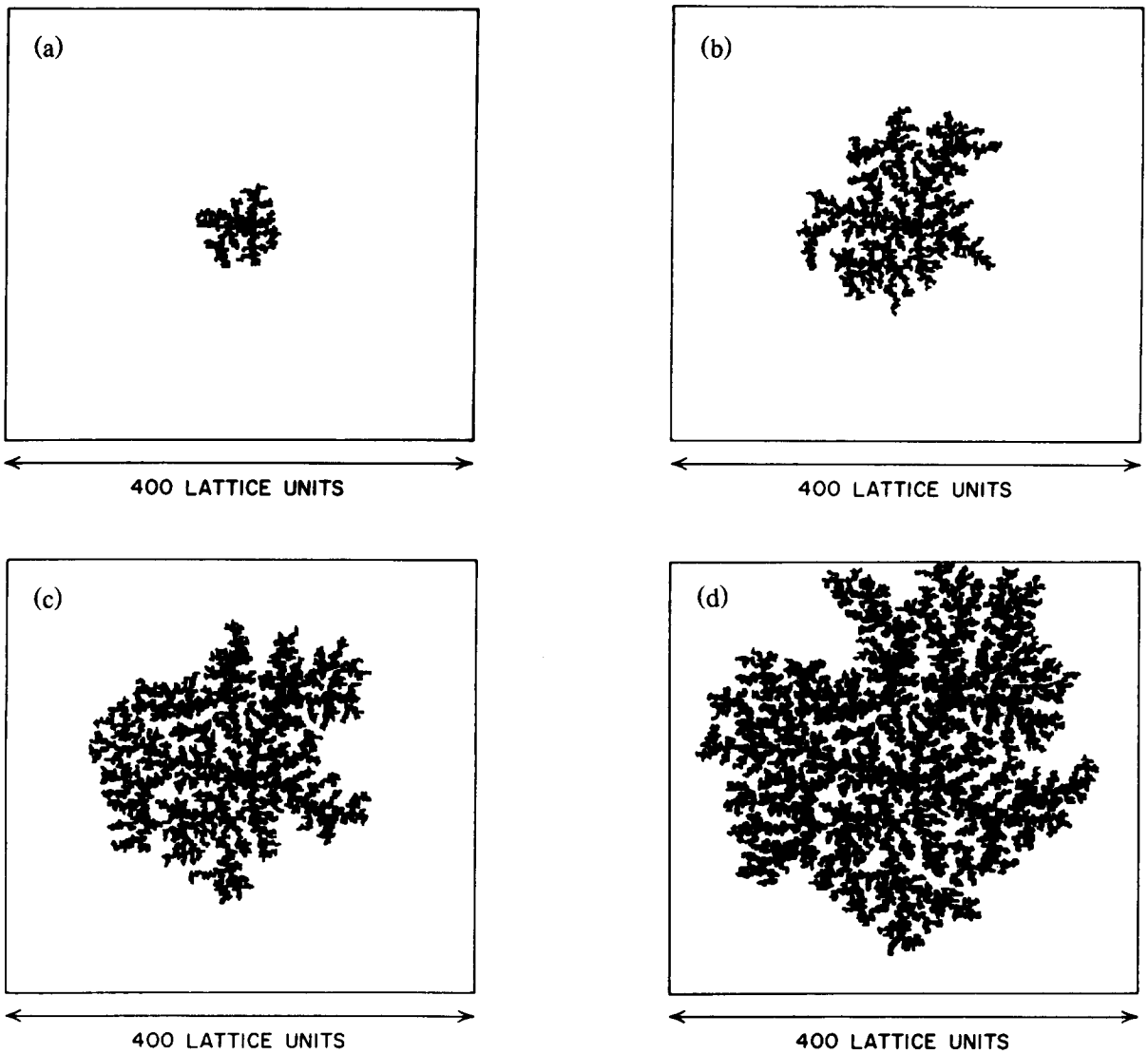

FIG. 2. This figure shows some of the results of a two-dimensional simulation in which 40 000 particles were added to a 400×400 lattice containing a single growth site at the center. (a) At the early stages of growth (1000 particles have been added in this figure) the cluster closely resembles a WS cluster. (b) At this stage 5000 particles have been added and the cluster is already considerably more compact than a WS cluster of 5000 particles. The average density of the cluster is now similar to the average concentration of the particles (0.25 particles per lattice site). (c) Ten thousand particles have now been added to the cluster which is uniform on all but quite short length scales. (d) Now 20 000 particles have been added (50% of the original 40 000 particles). The cluster is denser and considerably more uniform than the cluster of 20 000 particles shown in Fig. 1(d).

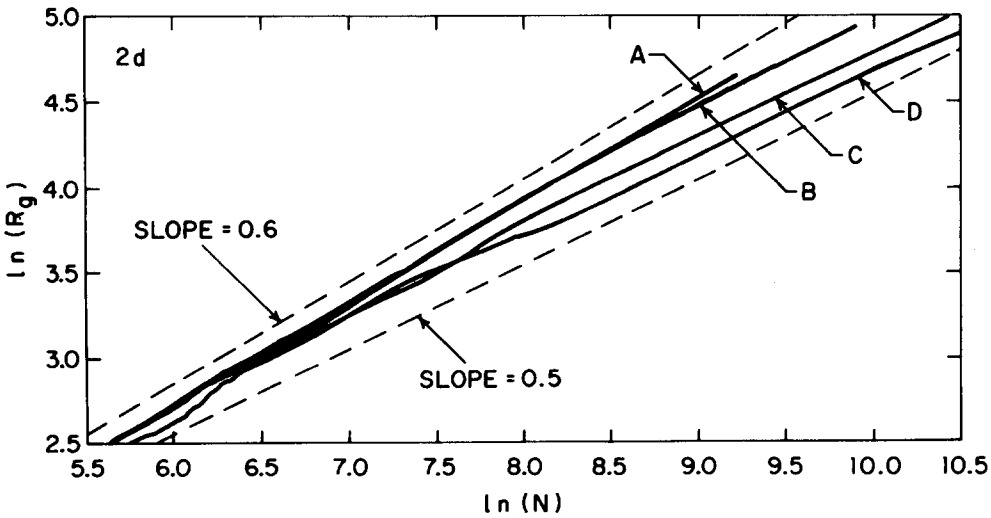

FIG. 3. Dependence of radius of gyration (R_g) on cluster size (N) for two-dimensional lattice models of diffusion limited aggregation in the form of log–log plots. The simulations were carried out on a 400×400 square lattice with one "seed" and a variable number of particles which were present at all times as either mobile particles or as part of the cluster grown from the seed. Curve A shows the results for 10 000 particles ($\rho = 0.0625$ particles per lattice site). For curve B, $\rho = 0.125$ (20 000 particles), for curve C, $\rho = 0.25$ (40 000 particles) and for curve D, $\rho = 0.3125$ (50 000 particles).

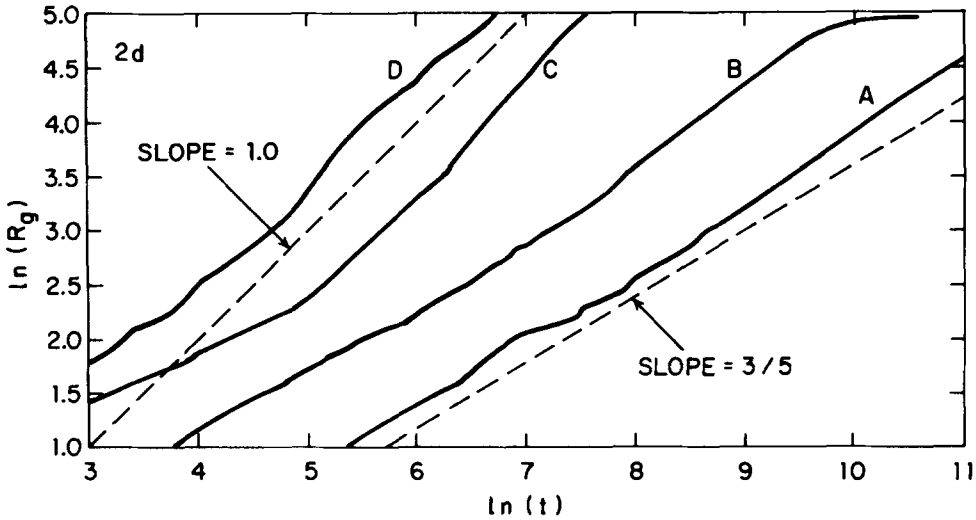

FIG. 4. This figure shows how the radius of gyration (R_g) increases with time. Curves A, B, C, and D were obtained using 10 000, 20 000, 40 000, and 50 000 particles, respectively, in the simulation. All simulations were carried out using a 400×400 square lattice. Curve D was obtained by averaging results from six simulations. "Time" is in units of Monte Carlo trials per particle.

sion controlled reacting systems when the concentration of reacting sinks is finite.[18]

B. Three dimensional simulations

Similar simulations have been carried out on a three dimensional lattice. The qualitative dependence of the radius of gyration on the cluster size is similar to that observed in two dimensional simulations. If the system is started out with a small particle concentration, the WS behavior persists until the late stages of the simulation, and we find that $R_g \sim N^{\beta}$ ($\beta \approx 0.4$). If the initial concentration of particles is large, there is a crossover from $\beta \approx 0.4$ to $\beta \approx 1/3$ during the early stages of growth.

Figure 7 shows the dependence of cluster size (N) on time (t) for simulations carried out on a $60 \times 60 \times 60$ cubic lattice with a single seed or growth site. To obtain curve D, 40 000 particles were added at the start of the simulation ($\rho = 0.185$). To obtain curves C, B, and A, the initial densities were set to 0.0926, 0.0463, and 0.0231 particles per lattice site, respectively. The results shown in curves B, C, and D in Fig. 7 are each taken from a single simulation, and curve A is the average of five simulations. The two dashed lines shown in Fig. 7 have slopes of 3.0 and 5/3 corresponding to Eqs. (4) and (8). At low particle concentrations, the clusters grow with the structure of three dimensional WS clusters and $N \sim t^{\delta}$ ($\delta \approx 5/3$). At high particle concentrations, the clusters have a uniform density distribution on all but very small length scales and $\delta \approx 3$. At intermediate densities, we would expect to see a crossover from $\delta \approx 5/3$ to $\delta \approx 3$. There is some evidence for this behavior, but we have not been able to carry out simulations on a large enough system to see $N \sim t^{5/3}$ and $N \sim t^{3}$ behavior at different stages in the *same* simulation.

The time dependence of the radius of gyration obtained from these simulations is shown in Fig. 8. For an initial concentration of 0.0231 particles per lattice site (curve A), we find that $R_g \sim t^{\eta}$ ($\eta \approx 2/3$) throughout much of the simulation, in good agreement with Eq. (3). In the case of a high initial particle concentration in the medium ($\rho = 0.185$ particles per lattice site for curve D), we find that $R_g \sim t^{\eta}$ ($\eta \approx 1.0$) in accord with Eq. (7). At intermediate concentrations (curves B and C), we observe intermediate behavior. The finite size of our simulations and statistical uncertainties

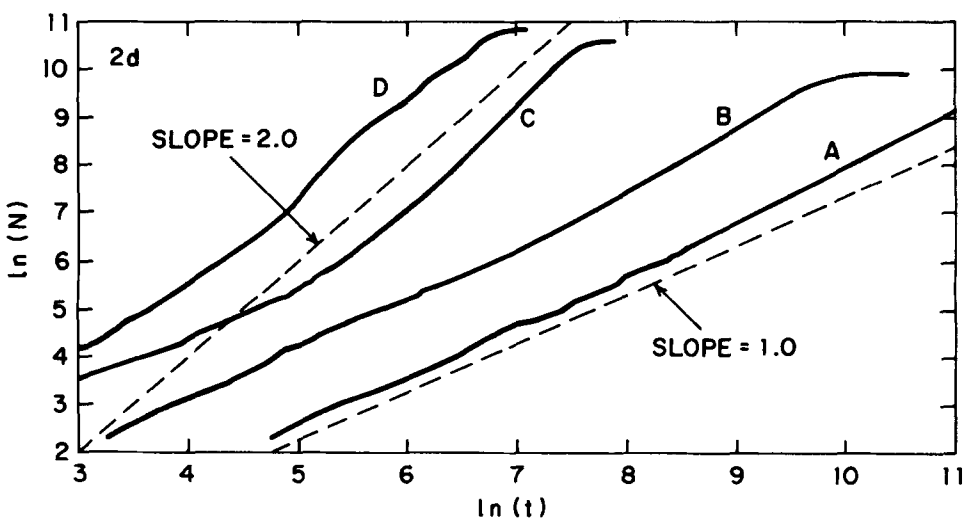

FIG. 5. Time dependence of the radius of gyration (R_g) for the two dimensional simulations used to obtain Figs. 3 and 4. Curve D was again obtained by averaging results from six simulations using 50 000 particles on a 400×400 lattice ($\rho = 0.3125$). The initial particle densities in the other simulations were 0.0625 for curve A, 0.125 for curve B, and 0.25 for curve C.

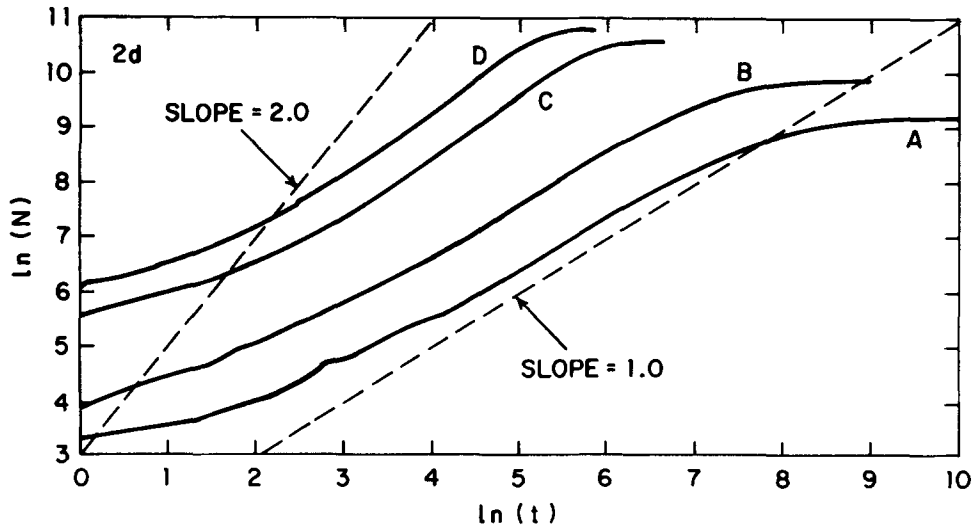

FIG. 6. Dependence of cluster mass (N) on Monte Carlo time for simulations in which 10 000 particles (curve A), 20 000 particles (curve B), 40 000 particles (curve C), and 50 000 particles were added to 50 growth sites randomly placed on a 400×400 lattice. The straight lines with slopes of 1.0 and 2.0 represent the limiting low and high concentration growth law for large isolated clusters.

make it difficult to draw conclusions from curves B and C, but in the region where statistical errors are smallest (large cluster sizes), the slope of curve B is closer to 2/3 and the slope of curve C is closer to 1.0.

The data presented in Fig. 8 indicate that $\eta \simeq 1.0$ at high concentrations ($\rho = 0.185$) and $\eta \simeq 2/3$ at relatively low concentrations (0.0231). It is possible that η would become even smaller at smaller concentrations. Consequently, similar simulations have been carried out at lower concentrations. Figure 9 shows the results obtained using 5000 mobile particles on $70\times70\times70$ lattices ($\rho = 0.0146$) and on $80\times80\times80$ lattices ($\rho = 0.00\,977$). The results shown in Figure 9 indicate that the limiting ($\rho \to 0$) value for the exponent η is close to 2/3.

IV. DISCUSSION

Diffusion limited aggregation has been simulated under conditions where all of the particles are present either as mobile particles or as part of a growing cluster. In early stages of the cluster growth when the cluster density is less than the medium density, this model is equivalent to the Witten–Sander model for diffusion limited aggregation.[1] Under these conditions, we find that the radius of gyration grows according to the growth law

$$R_g \sim t^{1/(2+D-d)}, \tag{9}$$

in agreement with our earlier results. Equation (9) implies that the time dependence of the number of particles in the cluster will be given by a power law relationship of the form

$$N \sim t^{D/(2+D-d)}. \tag{10}$$

Our simulations are in good agreement with Eq. (10) in two and three dimensions if $D \simeq 5/3$ for $d = 2$ and $D \simeq 5/2$ for $d = 3$.

At later stages of cluster growth when the cluster density has approached the medium density (below the percolation threshold), we find that

$$R_g \sim t \tag{11}$$

for $d = 2$ and 3. In this limit, the clusters have a uniform structure on all but very short length scales.

Under most circumstances (i.e., at intermediate concentrations), the initial stages produce WS clusters which grow according to Eqs. (9) and (10). As the clusters grow larger and larger, they become less and less dense until the density of the cluster approaches the density of the particles in the surrounding medium. At this stage there is a crossover from a

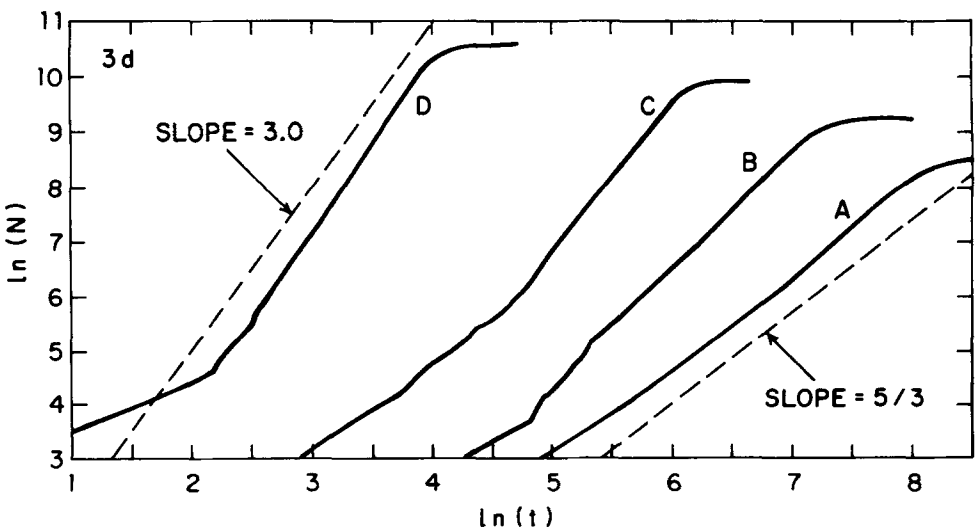

FIG. 7. Time dependence of total cluster size (N) during simulations in which particles were added to a single growth site on a $60\times60\times60$ lattice. The initial conditions were 5000 particles ($\rho = 0.0231$) for curve A, 10 000 particles ($\rho = 0.0463$) for curve B, 20 000 particles ($\rho = 0.0926$) for curve C, and 40 000 mobile particles ($\rho = 0.185$) for curve D. The limiting low concentration $N \sim t^{5/3}$ and high concentration $N \sim t^{3.0}$ behavior can be clearly seen in this figure.

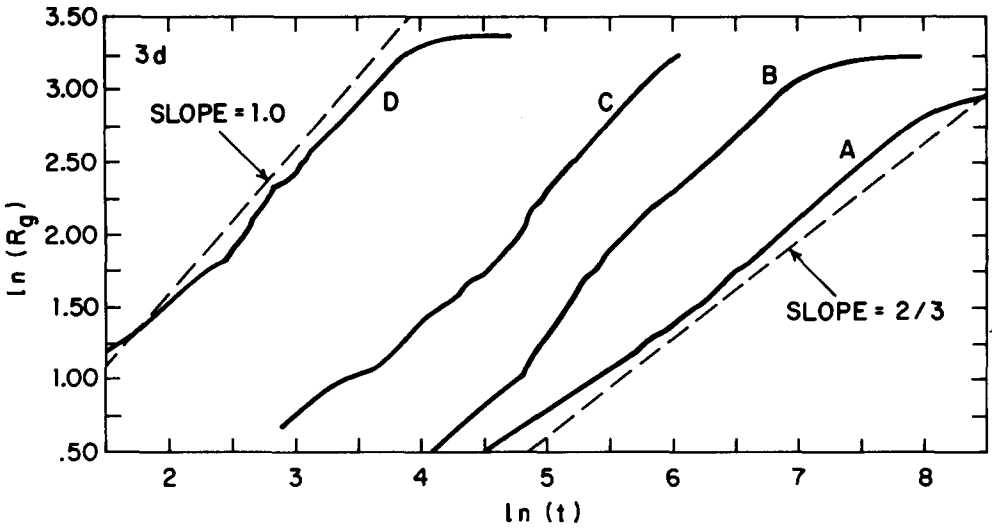

FIG. 8. This figure shows the time dependence of the radius of gyration calculated during the simulations used to obtain the results shown in Fig. 7. The concentrations used in these simulations were 0.0231 (curve A), 0.0463 (curve B), 0.0926 (curve C), and 0.185 (curve D) particles per lattice site.

growth exponent of $1/(2+D-d)$ (for R_g) to 1.0, and the Hausdorff dimensionality of the cluster crosses over from $D \simeq 5d/6$ to $D \simeq d$.

The crossover in the growth exponent is accompanied by a crossover in the process whereby particles are added to the growing cluster. The total flux of particles added to the cluster contains two contributions; the first is the diffusive flux (J_D).[15] The second contribution comes from the advance of the cluster "surface" into the surrounding medium (J_K). A rough estimate o f the contribution J_D is given by

$$J_D = A\delta\rho/R_g, \tag{12}$$

where A is the external area of the cluster and $\delta\rho$ is the difference between the concentration of particles in the bath and in the cluster. The second contribution to the flux of particles is given by

$$J_K = VA\rho_0, \tag{13}$$

where V is the velocity with which the surface is advancing and ρ_0 is the particle concentration (average concentration at long distances from the cluster). The total rate of growth of the cluster is given by

$$\frac{dN}{dt} = J_D + J_K. \tag{14}$$

At early stages of the cluster growth $J_D \gg J_K$, the diffusive flux is dominant and the system is in the regime discussed earlier.[15] At later stages of the cluster growth $\delta\rho \sim 0$ and $J_K \gg J_D \sim 0$ so the cluster surface, or interface, advances into the medium with a constant velocity.

The surprising success in two dimensions of the steady state diffusional picture on which our model is based deserves comment. The result $R(t) \sim t^{1/D}$ for $d=2$ appears to explain the simulation despite the fact that in two dimensions there is no steady state solution to the diffusion Eq. (2). For absorbing boundary conditions at R, the exact result for J_D is known to be

$$J_D(t) = \rho_0\left(\frac{8D}{\pi}\right)\int_0^\infty \frac{dk}{k} exp(-Dk^2t) \times [Y_0^2(kR) + J_0^2(kR)]^{-1}, \tag{15}$$

where Y_0 and J_0 are zeroth-order Bessel functions. In the long-time limit $J_D(t) \to (\ln t)^{-1}$ which, if employed in an analysis, would vitiate the result presented in Eq. (1). However, the short time limit leads to

$$J_D(t) \to \rho_0(\pi Dt)^{-1/2} A, \tag{16}$$

which in the early stages of growth predicts for a compact

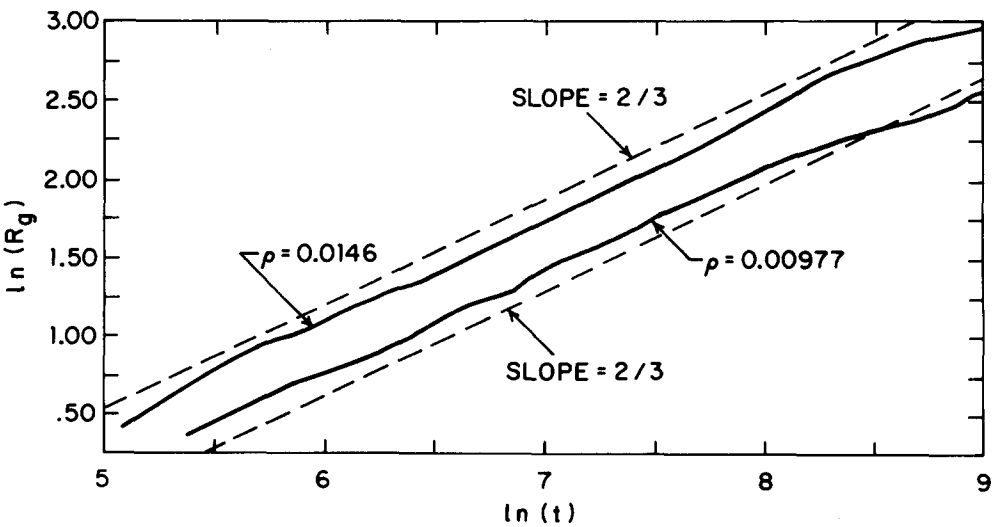

FIG. 9. Time dependence of the radius of gyration for clusters of 5000 particles each grown on $70\times70\times70$ ($\rho = 0.0146$) and $80\times80\times80$ ($\rho = 0.00977$) cubic lattices. The dashed line has a slope of 2/3 and represents our theoretical prediction. Curve A is the average of four simulations carried out on a $70\times70\times70$ lattice and curve B is the average of two simulations carried out on an $80\times80\times80$ lattice.

cluster in two dimensions the rate law

$$\frac{dN}{dt} = J_D(t) \sim N^{1/2}\ t^{-1/2}. \tag{17}$$

This short-time expression for $d = 2$ predicts $N(t) \sim t$. If we apply the result to a cluster of Hausdorff dimensionality D, we obtain $R_g(t) \sim t^{-1/D}$ in agreement with the $d = 2$ limit of Eq. (1). While this argument is helpful in providing an explanation for why our results work in two dimensions, it is far from rigorous. We believe that further work on two dimensional diffusion limited cluster growth is needed.

In this work, it has been assumed that the particles forming the aggregate follow diffusional (Brownian) trajectories with a Hausdorff dimensionality D_T of 2.0. However, the analysis can be generalized to cases where the particle trajectory has a Hausdorff dimensionality different from 2. For example, if the particles follow random linear trajectories ($D_T = 1.0$), we expect that the cluster growth rate will be given by

$$\frac{dN(t)}{dt} \sim R_g^{d-1} \tag{18}$$

or

$$R_g(t) \sim t^{1/(1+D-d)}. \tag{19}$$

Equations (15) and (16) are appropriate only if $d - D < 1$. If $D - d > 1$, the cluster is transparent to a linear trajectory. However, for this reason $d - D < 1$ if the cluster is generated by particles having linear trajectories. More generally if the particle trajectory has a fractal dimensionality of D_T, the growth law for the cluster will be given by

$$\frac{dN}{dt} \sim R_g^{(d-D_T)} \quad \text{and} \quad R_g \sim t^{1/(D_T+D-d)} \tag{20}$$

with the condition $D_T > (d - D)$.

A further generalization is possible if the medium in which the diffusion limited growth is occurring is itself a fractal structure. For example, for the case of diffusion limited aggregation on a random walk we have

$$N^2(t) \sim t, \quad R_g(N) \sim N^{1/2}, \quad R_g \sim t^{1/4}. \tag{21}$$

Another example would be diffusion limited aggregation on a percolation cluster.

We are in the process of carrying out simulations of diffusion limited aggregation with fractal particle trajectories and simulations of diffusion limited aggregation on fractal substrates such as percolation clusters.[19]

[1] T. A. Witten and L. M. Sander, Phys. Rev. Lett. **47**, 1400 (1981).
[2] P. Meakin, Phys. Rev. A **27**, 604, 1495 (1983).
[3] P. A. Rikvold, Phys. Rev. A **26**, 647 (1982).
[4] Y. Sawada, S. Ohta, M. Yamazaki, and H. Honjo, Phys. Rev. A **26**, 3557 (1982).
[5] P. Meakin, Phys. Rev. B **28**, 6718 (1983).
[6] H. Gould, H. E. Stanley, and F. Family, Phys. Rev. Lett. **50**, 686 (1983).
[7] M. Muthukumar, Phys. Rev. Lett. **50**, 839 (1983).
[8] M. Nauenberg, Phys. Rev. B **28**, 449 (1983).
[9] R. Ball, M. Nauenberg, and T. A. Witten (to be published).
[10] T. A. Witten and L. M. Sander, Phys. Rev. B **27**, 5686 (1983).
[11] M. Sahimi and G. R. Gerauld, J. Phys. A (to be published).
[12] C. Allain and B. Jouhier, J. Phys. Lett. **44**, L421 (1983).
[13] B. B. Mandelbrot *The Fractal Geometry of Nature* (Freeman, San Francisco, 1977).
[14] F. Hausdorff, Math. Annalen **79**, 157 (1919).
[15] J. M. Deutch and P. Meakin, J. Chem. Phys. **78**, 2093 (1983).
[16] T. A. Witten, Proceedings "MACRO 82" IUPAC, Amherst, Mass., June 1982, p. 88.
[17] T. A. Witten and P. Meakin, Phys. Rev. B **28**, 5632 (1983).
[18] See B. V. Felderhof, J. M. Deutch, and V. M. Titulaer, J. Chem. Phys. **76**, 4178 (1982), and references cited therein.
[19] P. Meakin (to be published).